J|A|C|S
ARTICLES
Published on Web 06/12/2003

A Cornucopia of Cycloadducts: Theoretical Predictions of the Mechanisms and Products of the Reactions of Cyclopentadiene with Cycloheptatriene

Andrew G. Leach,[†] E. Goldstein,[‡] and K. N. Houk*,[†]

Contribution from the Department of Chemistry and Biochemistry, University of California, Los Angeles, California 90095, and Department of Chemistry, California State Polytechnic University at Pomona, 3801 West Temple Avenue, Pomona, California 91768

Received December 11, 2002; E-mail: houk@chem.ucla.edu

Abstract: The potential cycloaddition reactions between cyclopentadiene and cycloheptatriene have been explored theoretically. B3LYP/6-31G* was used to locate the transition states, intermediates, and products for concerted pathways and stepwise pathways passing through diradical intermediates. Interconversions of various cycloadducts through sigmatropic shifts were also explored. CASPT2/6-31G* single point calculations were employed to obtain independent activation energy estimates. MM3 was also used to compute reaction energetics. Several bispericyclic cycloadditions in which two cycloadducts are linked by a sigmatropic shift have been identified. B3LYP predicts, in line with frontier molecular orbital predictions, that the [6+4] cycloaddition is the favored concerted pathway, but an alternative [4+2] pathway is very close in energy. By contrast, CASPT2 predicts that a [4+2] cycloaddition is the preferred pathway. B3LYP predicts that the lowest energy path to many of the cycloadducts will involve diradical intermediates, whereas CASPT2 predicts that each of the products of orbital symmetry allowed reactions will be reached most readily by closed shell processes—concerted cycloadditions and sigmatropic shift rearrangements of cycloadducts.

Introduction

In the Fall of 1964, one of the current authors, K. N. Houk, made his third visit to R. B. Woodward's office at Harvard to talk about potential Ph.D. projects. Professor Woodward told the young man, "Roald Hoffmann and I have predicted that the [6+4] cycloaddition should occur.[1] Why not look for one? The reaction of cycloheptatriene and cyclopentadiene would be a good place to start." (Scheme 1). Woodward and Hoffmann also predicted that the [6+4] cycloaddition should be exo, in contrast to the oft-observed endo stereoselectivity of the Diels−Alder reaction.[2,3] In the course of Houk's graduate work, several [6+4] cycloadditions and many more [4+2] cycloadditions were found with substituted dienes and trienes,[4] but the many products of the thermal reaction of cycloheptatriene and cyclopentadiene, detected by gas chromatographic analysis of the reaction mixture, were never characterized.[5]

We have now used modern quantum mechanical calculation methods to solve this problem, at least theoretically, nearly 40 years after it was proposed by Woodward. The experimental investigation remains an "amusing" Ph.D. project, and the computational results here provide a detailed road map for an experimentalist who chooses to take up Woodward's challenge in the future.

Scheme 1. [6+4] Cycloaddition of Cycloheptatriene and Cyclopentadiene

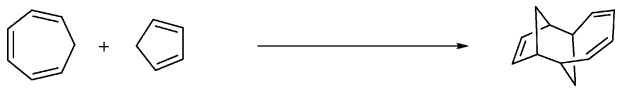

Frontier molecular orbital (MO) considerations lead to the expectation that the [6+4] cycloaddition should proceed in preference to alternative cycloaddition types.[6] As shown in Figure 1, whether the reaction is under HOMO (cycloheptatriene)−LUMO (cyclopentadiene) or HOMO (cyclopentadiene)−LUMO (cycloheptatriene) control, the large orbital coefficients at the termini of the polyenes favor the [6+4] cycloaddition.

In addition to the [6+4] cycloaddition, four allowed [4+2] cycloadditions (reactions 2−5, Figure 2) or forbidden [2+2], [4+4], or [6+2] cycloadditions (reactions 6−10, Figure 2) are possible. Each of these reactions may proceed to endo or exo products. The two reactants can also dimerize rather than reacting with the other component. For example, cyclopentadiene dimerizes to the endo Diels−Alder (or [4+2]) dimer, with

[†] University of California, Los Angeles.
[‡] California State Polytechnic University at Pomona.

(1) This prediction appeared in: Hoffmann, R.; Woodward, R. B. *J. Am. Chem. Soc.* **1965**, *87*, 2046−2048.
(2) Hoffmann, R.; Woodward, R. B. *J. Am. Chem. Soc.* **1965**, *87*, 4388−4389.
(3) Woodward, R. B.; Hoffmann, R. *Angew. Chem., Int. Ed. Engl.* **1969**, *8*, 781; *The Conservation of Orbital Symmetry*; Verlag Chemie: Weinheim, 1970.
(4) (a) Houk, K. N.; Woodward, R. B. *J. Am. Chem. Soc.* **1970**, *92*, 4143−4145. (b) Houk, K. N.; Woodward, R. B. *J. Am. Chem. Soc.* **1970**, *92*, 4145−4147.(c) Bhacca, N. S.; Luskus, L. J.; Houk, K. N. *Chem. Commun.* **1971**, 109−111.
(5) Houk, K. N. Ph.D. Thesis, Harvard University, Cambridge, MA, 1964.
(6) (a) Fleming, I. *Frontier Orbitals and Organic Chemical Reactions*; Wiley & Sons: New York, 1996; p 173. (b) Mukherjee, D.; Watts, C. R.; Houk, K. N. *J. Org. Chem.* **1978**, *43*, 817−821.

10.1021/ja029694x CCC: $25.00

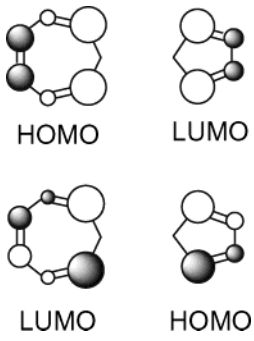

Figure 1. Frontier molecular orbitals of cycloheptatriene and cyclopentadiene.

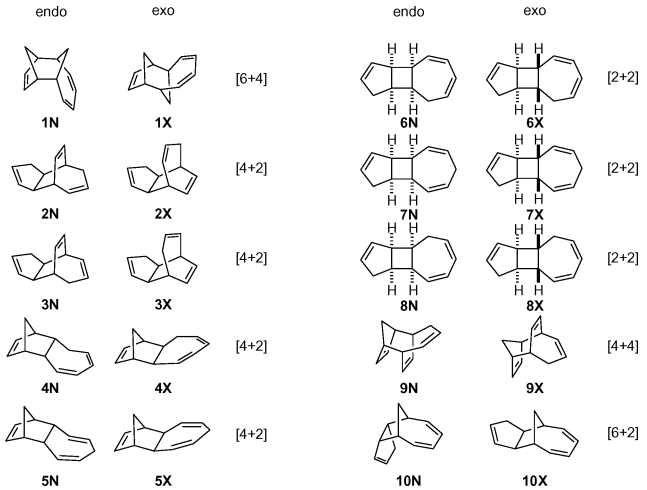

Figure 2. Products of cycloaddition reactions of cyclopentadiene and cycloheptatriene. Orbital symmetry allowed reactions are shown in the left-hand column and forbidden reactions to the right.

none of the [2+2] or [4+4] adducts.[7] Cycloheptatriene is known to isomerize to norcaradiene and to undergo a range of cycloadditions.[4,5,8] Oligomers can also form by successive Diels−Alder reactions.

It is now known that concerted thermally allowed reactions often compete with stepwise processes that can lead to either allowed or forbidden products. Many calculations have been reported on the related reactions of butadiene and ethylene[9] and the dimerization reactions of cyclobutadiene[10] and cyclopentadiene.[11] In the study of the mechanism of the Diels−Alder reaction of butadiene and ethylene,[9] the lowest energy stepwise pathway was found to have a free energy of activation ranging between 2.3 and 7.7 kcal/mol above the concerted path. B3LYP/6-31G* energies and geometries agreed well with experimental results. Calculated secondary kinetic isotope effects for more substituted Diels−Alder reactions support a concerted mechanism and match experimental data.[9g,h,12]

Caramella recently studied the dimerization of cyclopentadiene with B3LYP/6-31G* and discovered that the preferred reaction path involves a bispericyclic transition state.[11] A transition state was found where two [4+2] cycloaddition reactions are merged; the transition state is symmetrical and both cycloadditions have proceeded to the same (asynchronous) degree. Motion toward products leads along the symmetrical path toward a second transition state, with the same symmetry, which is that of a Cope rearrangement linking the two alternative cycloadducts. A valley−ridge inflection intervenes as the second stage of the cycloaddition reaction and is the point at which the reaction trajectory must break symmetry and select one of the two cycloaddition pathways.

A number of formally forbidden reactions may also be expected to occur in the cycloheptatriene−cyclopentadiene reaction, since the reactants may be expected to undergo stepwise reactions involving the intermediacy of stabilized diradicals, **11**. The Woodward−Hoffmann rules of orbital

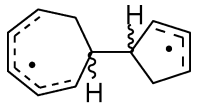

11

symmetry do not apply to such stepwise processes, but we have recently shown that orbital symmetry can influence the barriers to cyclization of diradicals.[13]

We have performed a B3LYP/6-31G* study of the reaction between cyclopentadiene and cycloheptatriene. Where appropriate, CASPT2/6-31G* single point calculations were performed on the B3LYP geometries. We have discovered that concerted and stepwise reactions are very close in energy and that formally forbidden and allowed cyclizations of diradicals are also close in energy.

Computational Methods

B3LYP/6-31G* calculations[14−16] were performed with the Gaussian 98 suite of programs.[17] CASPT2 calculations were performed with the MOLCAS suite of programs.[18] These methods have recently been shown to be accurate methods for the prediction of activation barriers for pericyclic reactions of hydrocarbons.[19] Constrained optimizations

(7) (a) Alder, K.; Stein, G. *Liebigs Ann. Chem.* **1933**, *504*, 216−257. (b) Alder, K.; Stein, G. *Angew. Chem.* **1934**, *47*, 837−848. (c) Alder, K.; Stein, G. *Angew. Chem.* **1937**, *50*, 510−519.
(8) (a) Maier, G. *Angew. Chem., Int. Ed. Engl.* **1967**, *6*, 402. (b) Kresze, G.; Schulz, G. *Tetrahedon* **1961**, *12*, 7−12. (c) Hutton, J.; Waters, W. A. *Chem. Commun.* **1966**, 634. (d) Leitich, J.; Sprintschnik, G. *Chem. Ber.* **1986**, 1640. (e) Fray, G. I. *J. Chem. Soc.* **1963**, 4284−4285.
(9) (a) Caramella, P.; Domelsmith, L. N.; Houk, K. N. *J. Am. Chem. Soc.* **1977**, *99*, 4511−4514. (b) Brown, F. K.; Houk, K. N. *Tetrahedron Lett.* **1984**, *25*, 4609−4612. (c) Houk, K. N.; Lin, Y. T.; Brown, F. K. *J. Am. Chem. Soc.* **1986**, *108*, 554−556. (d) Li, Y.; Houk, K. N. *J. Am. Chem. Soc.* **1993**, *115*, 7478−7485. (e) Houk, K. N.; Yi, L.; Storer, J.; Raimondi, L.; Beno, B. *J. Chem. Soc., Faraday Trans.* **1994**, *90*, 1599−1604. (f) Storer, J. W.; Raimondi, L.; Houk, K. N. *J. Am. Chem. Soc.* **1994**, *116*, 9675−9683. (g) Goldstein, E.; Beno, B.; Houk, K. N. *J. Am. Chem. Soc.* **1996**, *118*, 6036−6043. (h) Beno, B. R.; Houk, K. N.; Singleton, D. A. *J. Am. Chem. Soc.* **1996**, *118*, 9984−9985.
(10) (a) Li, Y.; Houk, K. N. *J. Am. Chem. Soc.* **1996**, *118*, 880−885. (b) Limanto, J.; Tallarico, J. A.; Porter, J. R.; Khuong, K. S.; Houk, K. N.; Snapper, M. L. *J. Am. Chem. Soc.* **2002**, *124*, 14748−14758.
(11) Caramella, P.; Quadrelli, P.; Toma, L. *J. Am. Chem. Soc.* **2002**, *124*, 1130−1131.
(12) Wiest, O.; Montiel, D. C.; Houk, K. N. *J. Phys. Chem. A* **1997**, *101*, 8378−8388.
(13) Leach, A. G.; Catak, S.; Houk, K. N. *Chem. Eur. J.* **2002**, *8*, 1290−1299.
(14) (a) Becke, A. D. *J. Chem. Phys.* **1993**, *98*, 1372−1377. (b) Becke, A. D. *J. Chem. Phys.* **1993**, *98*, 5648−5652. (c) Stephens, P. J.; Devlin, F. J.; Chabalowski, C. F.; Frisch, M. J. *J. Phys. Chem.* **1994**, *98*, 11623−11627.
(15) Lee, C.; Yang, W.; Parr, R. G. *Phys. Rev. B* **1988**, *37*, 785−789.
(16) Hariharan, P. C.; Pople, J. A. *Theor. Chim. Acta* **1973**, *28*, 213−222.
(17) Frisch, M. J.; Trucks, G. W.; Schlegel, H. B.; Scuseria, G. E.; Robb, M. A.; Cheeseman, J. R.; Zakrzewski, V. G.; Montgomery, J. A.; Stratmann, R. E.; Burant, J. C.; Dapprich, S.; Millam, J. M.; Daniels, A. D.; Kudin, K. N.; Strain, M. C.; Farkas, O.; Tomasi, J.; Barone, V.; Cossi, M.; Cammi, R.; Mennucci, B.; Pomelli, C.; Adamo, C.; Clifford, S.; Ochterski, J.; Petersson, G. A.; Ayala, P. Y.; Cui, Q.; Morokuma, K.; Malick, D. K.; Rabuck, A. D.; Raghavachari, K.; Foresman, J. B.; Cioslowski, J.; Ortiz, J. V.; Stefanov, B. B.; Liu, G.; Liashenko, A.; Piskorz, P.; Komaromi, I.; Gomperts, R.; Martin, R. L.; Fox, D. J.; Keith, T.; Al-Laham, M. A.; Peng, C. Y.; Nanayakkara, A.; Gonzalez, C.; Challacombe, M.; Gill, P. M. W.; Johnson, B. G.; Chen, W.; Wong, M. W.; Andres, J. L.; Head-Gordon, M.; Replogle, E. S.; Pople, J. A. *Gaussian 98*, Revision A.7; Gaussian, Inc.: Pittsburgh, PA, 1998.

were performed using redundant internal coordinates in Gaussian 98. Open shell singlet diradicals were optimized starting from an initial guess for the wave function in which the HOMO and LUMO are mixed. Spin projection on the resulting spin-contaminated species employed the method of Yamaguchi et al.[20] MM3[21] calculations were performed with MacroModel.[22]

Energies quoted incorporate unscaled zero point energy corrections based on unscaled B3LYP/6-31G* frequencies. Frequency calculations verified the identity of minima, transition states, and second-order saddle points.

Nomenclature Issues

All possible products of allowed cycloadditions are shown on the left-hand side of Figure 2. These are **1** [6+4], **2** [4+2], **3** regioisomeric [4+2], **4** [2+4] on a terminal double bond of cycloheptatriene, and **5** [2+4] on the internal double bond of cycloheptatriene. The products of Woodward−Hoffmann forbidden cycloadditions are shown on the right-hand side of Figure 2. These include various [2+2], [4+4], and [6+2] processes. Only suprafacial cycloadditions are considered.

Products are labeled with the corresponding reaction number and either **N**, for the endo adduct, or **X** for the exo adduct. Thus, the [6+4] exo cycloadduct is labeled **1X**. Concerted cycloaddition transition states are labeled according to the product of the reaction and then **CTS**, to indicate concerted transition state. Thus, the transition state for the concerted exo [6+4] cycloaddition is labeled **1XCTS**. Diradicals may be either syn or anti and are thus labeled with a number and either **S** or **A**. Similar labels are given for the transition states for formation of the diradicals. The transition states for diradical cyclization are labeled with the reaction number from Figure 2 and **X** or **N**, followed by **DRTS** (for diradical transition state). Thus the transition state in which the syn diradical **11S** cyclizes to yield the [6+4] exo cycloadduct is labeled **1XDRTS**. The transition states for the sigmatropic shift which links two alternative cycloadducts is labeled according to the two cycloadducts followed by **SSTS** (for sigmatropic shift transition state). Thus, the sigmatropic shift transition state linking **2N** and **4N** is labeled **2N4NSSTS**. We have no illusions about the generality of such nomenclature but hope that it provides a way for the reader to negotiate the complexities of this paper.

Results

The heat of formation of each of the cycloaddition products was computed with MM3 and B3LYP/6-31G*. The structures and energies obtained are included in the Supporting Information. B3LYP/6-31G* energetics have been incorporated into the reaction profiles accompanying the discussion of each reaction below. MM3 and B3LYP agree to a great extent on the thermodynamic endo−exo preferences. Both methods predict that the thermodynamically most favored reaction is that leading to the exo [6+2] product, **10X**. The [6+4] exo product **1X** is a close second by MM3, but higher in energy than several endo or exo [4+2] adducts according to B3LYP. B3LYP indicates that many of the reactions are approximately thermoneutral or endothermic, so that thermal equilibration of products should occur.

Table 1. Energies of Diradicals Calculated by B3LYP/6-31G* (with and without Spin Projection) and by CASPT2/6-31G*//B3LYP/6-31G*

diradical	ΔH_{rxn}(diradical) B3LYP	$\langle S^2 \rangle$	ΔH_{rxn}(diradical) spin-projected B3LYP	ΔH_{rxn}(diradical) CASPT2
11A	18.3	1.06	17.9	12.5
11S	18.5	1.06	18.0	13.7
12A	30.1	1.04	29.6	−[a]
12S	30.2	1.05	29.9	−[a]
13A	32.0	1.01	30.6	−[a]
13S	31.7	1.05	31.9	−[a]

[a] Not calculated.

B3LYP was used to optimize the concerted transition states for each of the allowed reactions. The structures of each transition state will be presented in the relevant sections below. The activation enthalpies for concerted formation of **1N**, **2N**, and **3N** could not be calculated since these cycloadducts could only be accessed through Cope rearrangements of **2X**, **4N**, and **5N**, respectively. These features will be discussed in more detail in the relevant section of the discussion.

The stepwise pathways involving diradical intermediates were also investigated. There are six diradical intermediates that are most likely to play a part in the reaction mechanism—a number of others include less resonance stabilization of one or both of the radical centers. The enthalpy of reaction on diradical formation was calculated for each of these six diradicals **11**−**13** (each of which may be syn or anti) and is displayed in Table

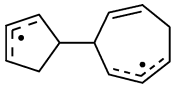

12

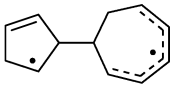

13

1. Singlet diradicals treated with UB3LYP are highly spin contaminated and usually have $\langle S^2 \rangle \approx 1$ involving near-degeneracy of singlet and triplet states. In such cases, spin projection by the method of Yamaguchi et al. was performed.[20]

Due to concerns about the reliability of B3LYP for prediction of the relative energies of restricted and unrestricted pathways,[23] CASPT2 single point energy evaluations were computed for each important structure. These calculations, performed with MOLCAS 5.0,[18] apply a second order perturbation theory correction to a CASSCF energy evaluation. The CASSCF calculation utilized an active space incorporating the six π electrons of cycloheptatriene and the corresponding π and π^* orbitals along with the four π electrons and orbitals of cyclopentadiene. The electrons and orbitals corresponding to these in each of the other structures were selected for the active space. The energies, including the B3LYP zero point energy correction, are indicated in each of the tables.

(18) Andersson, K.; Barysz, M.; Bernhardsson, A.; Blomberg, M. R. A.; Cooper, D. L.; Fleig, T.; Fülscher, M. P.; de Graaf, C.; Hess, B. A.; Karlström, G.; Lindh, R.; Malmqvist, P.-Å.; Neogrády, P.; Olsen, J.; Roos, B. O.; Sadlej, A. J.; Schütz, M.; Schimmelpfennig, B.; Seijo, L.; Serrano-Andrés, L.; Siegbahn, P. E. M.; Stålring, J.; Thorsteinsson, T.; Veryazov, V.; Widmark, P.-O. *MOLCAS*, Version 5; Lund University: Sweden 2000.
(19) Guner, V.; Leach, A. G.; Khuong, K. S.; Bartberger, M. D.; Lee, P. S.; Houk, K. N. Manuscript in preparation.
(20) Yamaguchi, K.; Jensen, F.; Dorigo, A.; Houk, K. N. *Chem. Phys. Lett.* **1988**, *149*, 537−542.
(21) Allinger, N. L.; Yuh, Y. H.; Lii, J.-H. *J. Am. Chem. Soc.* **1989**, *111*, 8551−8566 and subsequent additions.
(22) MacroModel V7.1, copyright Columbia University 1986−1998, Schrodinger Inc. 1999. Mohamadi, F.; Richards, N. G. J.; Guida, W. C.; Liskamp, R.; Lipton, M.; Caufield, C.; Chang, G.; Hendrickson, T.; Still, W. C. *J. Comput. Chem.* **1990**, *11*, 440−467.
(23) Staroverov, V. N.; Davidson, E. R. *J. Am. Chem. Soc.* **2000**, *122*, 186−187.

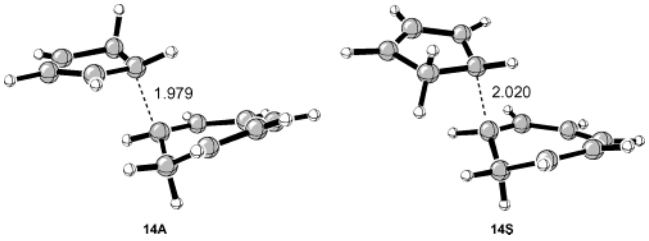

Figure 3. Transition states for the formation of diradicals **11A** and **11S** from cycloheptatriene and cyclopentadiene.

Table 2. Activation Energies for Formation of Diradicals **11A** and **11S**

diradical	$\Delta H^{\ddagger}$(diradical formation) B3LYP	$\langle S^2 \rangle$	$\Delta H^{\ddagger}$(diradical formation) spin-projected B3LYP	$\Delta H^{\ddagger}$(diradical formation) CASPT2
11A	28.7	0.49	24.7	21.6
11S	32.0	0.63	27.5	25.9

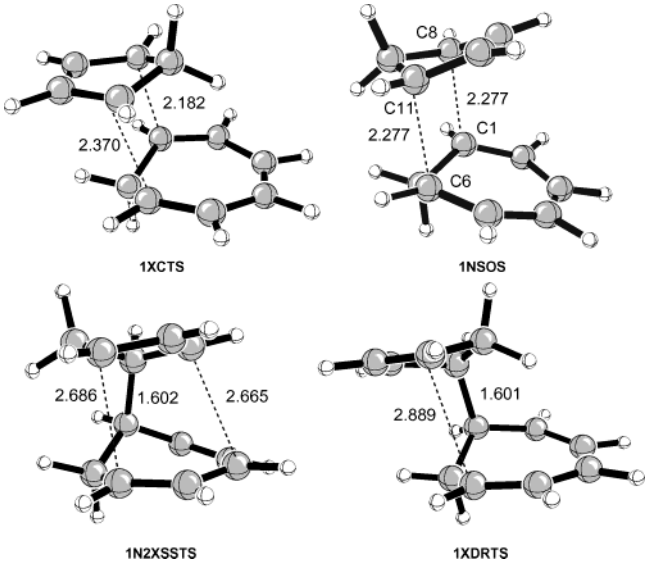

Figure 4. Transition states involved in the formation of **1X** and **1N**.

As is clear from Table 1, the maximally conjugated diradicals **11A** and **11S** are considerably lower in energy than the alternative diradicals **12** and **13**. The latter are all higher in energy than any of the concerted transition states. We have therefore considered in detail only those reactions that can take place through **11A** or **11S**. We have located the transition states **14A** and **14S** that link **11A** and **11S** to reactants, and these are shown in Figure 3. The enthalpies of these transition states, along with their spin-projected values, are shown in Table 2.

The diradicals may subsequently cyclize to yield one of the cycloadducts. Diradical **11A** may yield **1N**, **6N**, **9N**, **2X**, **4X**, and **10X**. Diradical **11S** on the other hand may lead to **2N**, **4N**, **10N**, **1X**, **6X**, and **9X**. The high energy diradical **12A** would be the lowest energy diradical en route to **7N**, **3X**, and **5X**. In each case, the opposite stereoisomer of the product (endo or exo) would be accessed through diradical **12S**. Diradicals **13A** and **13S** are the most likely diradicals to lead to **8X** and **8N**, respectively. Calculations predict that the diradical stepwise routes are only likely to be relevant to the overall product mixture for reactions leading to **1**, **2**, **4**, **6**, **9**, and **10**, all of which involve diradicals **11A** and **11S**. In the discussion below, spin-projected energies are used. The details are shown in the Supporting Information. The reactions that proceed through diradicals **11A** and **11S** all have in common that the transition state for diradical formation is the highest point on the reaction profile.

Discussion

In the following sections, each of the possible cycloadditions will be described, and the transition states and intermediates located for each will be discussed. Throughout the discussion below, the spin-projected values for the energies of the diradicals and the transition states leading to or from them will be used. These values are better in line with those calculated by CASPT2, as has been observed previously.[13]

1: The [6+4] Cycloaddition. Restricted B3LYP calculations identified only one concerted transition state for the [6+4]

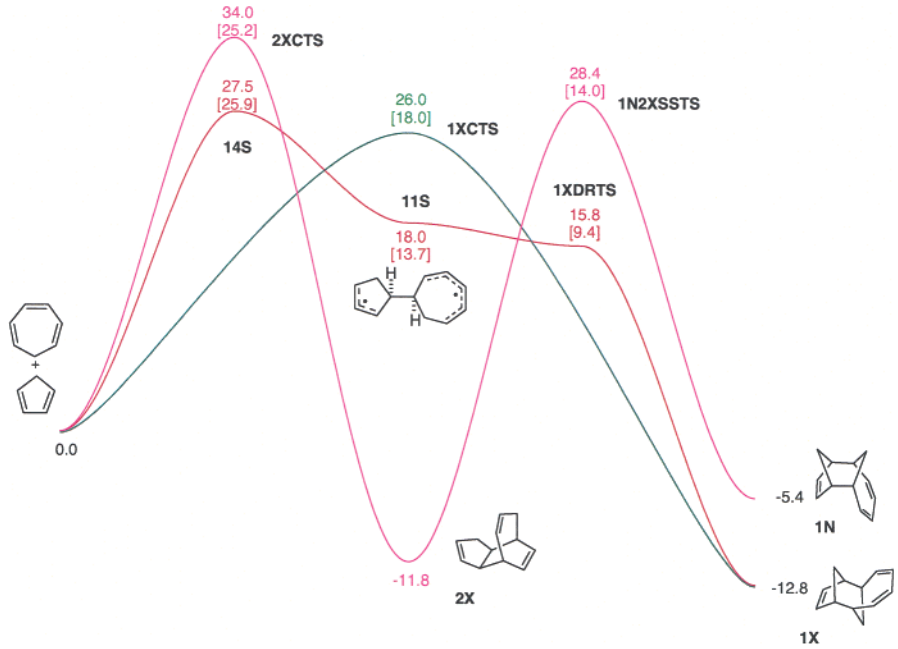

Figure 5. B3LYP/6-31G* [CASPT2/6-31G*] energetics for the cycloadditions leading to **1N** and **1X**.

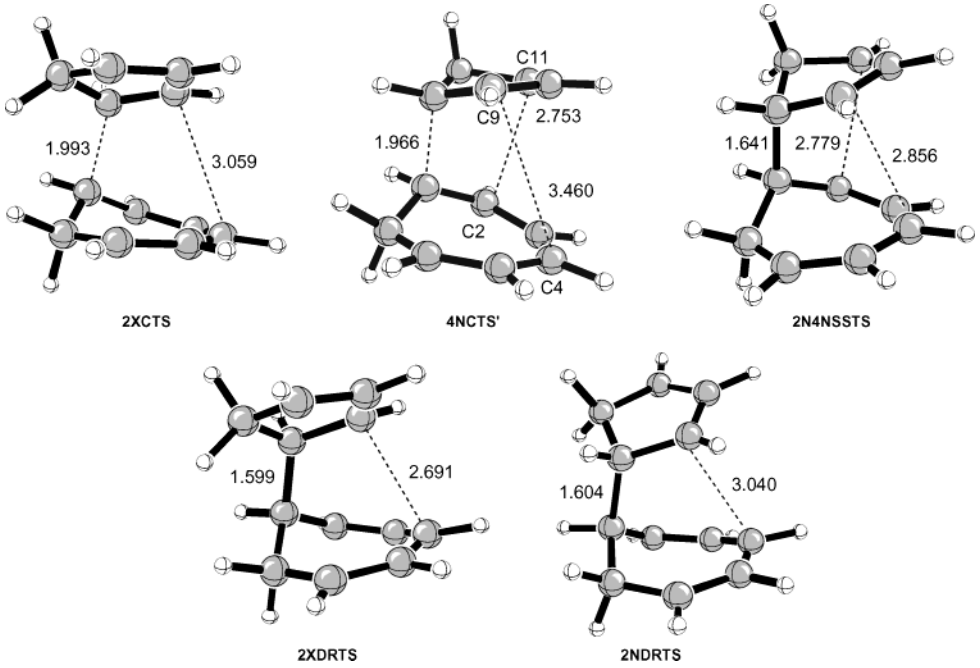

Figure 6. Transition states involved in the formation of **2X** and **2N**.

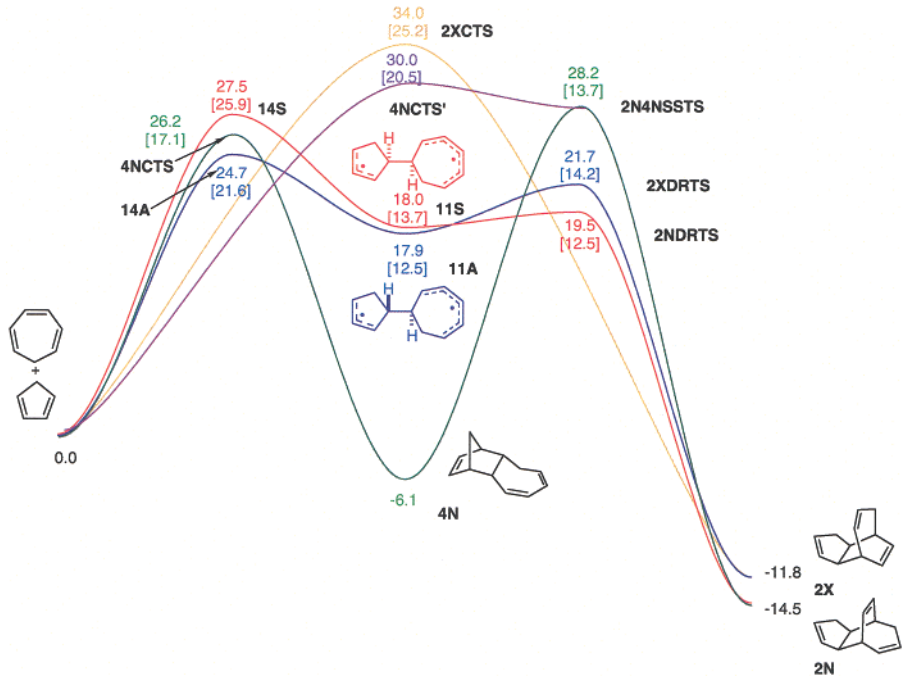

Figure 7. B3LYP/6-31G* [CASPT2/6-31G*] energetics for the cycloadditions leading to **2N** and **2X**. The purple curve signifying **4NCTS′** is shown to merge with the green curve showing the minimum energy path to **2N**. This represents the possibility afforded by the shape of the potential energy surface for trajectories to pass through **4NCTS′** to **2N** (via the region of **2N4NSSTS**) as well as to **4N**.

cycloaddition between cycloheptatriene and cyclopentadiene, the asynchronous exo **1XCTS** (Figure 4) at 26.0 kcal/mol relative to reactants and with forming bond lengths of 2.182 and 2.370 Å. When constrained to be synchronous, the energy increased by 5.8 kcal/mol and a second imaginary frequency vibration corresponding to symmetry breaking was computed. The forming bond lengths of this second-order saddle point were 2.268 Å, intermediate between those of the fully optimized structure.[24] The activation energy of 26.0 kcal/mol is the lowest

(24) Goldstein, E.; Beno, B. R.; Houk, K. N. *Theor. Chem. Acc.* **1999**, *103*, 81−84.

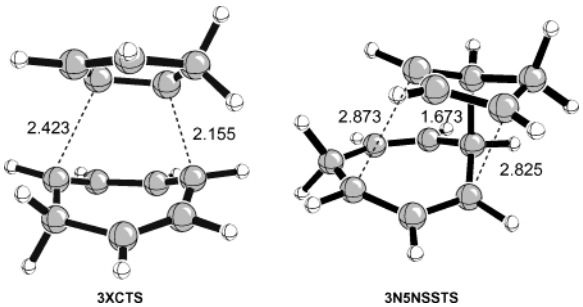

Figure 8. Transition states involved in the formation of **3X** and **3N**.

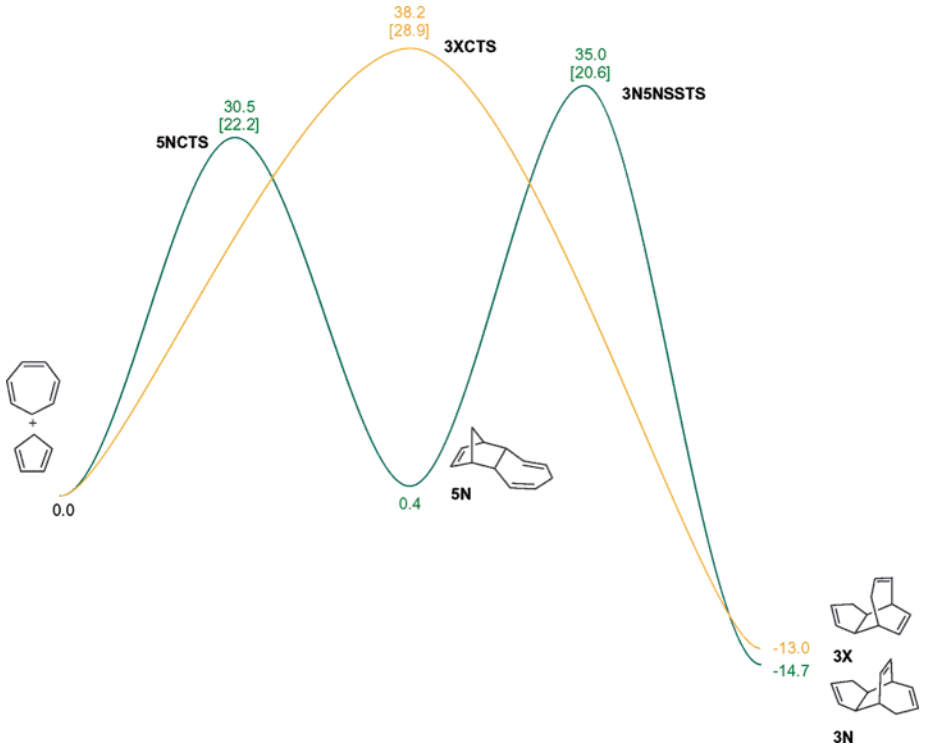

Figure 9. B3LYP/6-31G* [CASPT2/6-31G*] energetics for the cycloadditions leading to **3N** and **3X**.

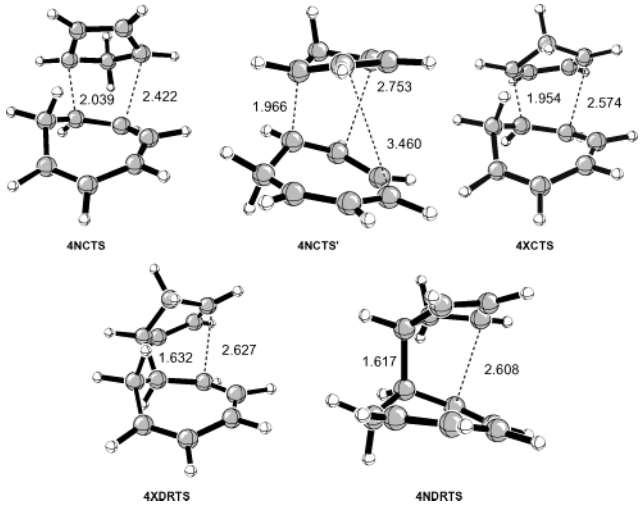

Figure 10. Transition states involved in the formation of **4N** and **4X**.

of all of the concerted pathways in line with the FMO prediction of a [6+4] cycloaddition and R. B. Woodward's intuition. The asynchronicity presumably reflects the considerable contribution of diradicals to the electronic structure of even the closed shell structures.

A concerted transition state for the endo cycloaddition stereochemistry could not be located. Optimization with C_S symmetry located a second-order saddle point, **1NSOS** at 37.0 kcal/mol relative to reactants with the two negative force constants corresponding to cycloaddition and a rocking motion corresponding to symmetry breaking. To establish more thoroughly the characteristics of this [6+4] endo cycloaddition transition state, a potential energy surface was generated using constrained optimizations. The two forming C−C bond distances (C1−C8 and C6−C11) were the coordinates used (see Supporting Information). This revealed that cycloadduct **1N** can be formed indirectly via one of the [4+2] cycloadducts, **2X**, followed by a [3,3] sigmatropic shift through a very loose, or dissociative, transition state **1N2XSSTS**, which B3LYP places at 28.4 kcal/mol relative to reactants. The initial formation of **2X** has a barrier of 34.0 kcal/mol. We were not able to locate a transition state for cyclization of a diradical leading to **1N** with unrestricted calculations. The large steric hindrance of the two CH_2 groups and the repulsive secondary orbital interaction between π systems disfavor direct pathways to the endo [6+4] adduct.

A stepwise pathway for the exo cycloaddition was found. The transition state for cyclization of diradical **11S**, **1XDRTS**, is 0.7 kcal/mol above the diradical or 2.2 kcal/mol lower in energy than the diradical after including zero point energy corrections. The diradical is in such a shallow well that the barriers to rotation about the C1−C8 bond in the diradical are larger than for cyclization (see Supporting Information). The diradical formation process is rate limiting in each of the stepwise processes described in this paper, and it is likely that the dynamic behavior of the system will play a role in determining the cyclization modes for each diradical.

The energetics for the [6+4] cycloaddition are summarized in Figure 5. Subsequent CASPT2 single point energy evaluations are also indicated in Figure 5 in brackets. The concerted exo cycloaddition is the lowest energy pathway. This is in line with the thermodynamic preference for the reaction and with the Woodward−Hoffmann prediction.

With CASPT2, the energetics are considerably different: the diradicals are lowered, but the transition state for diradical formation is only 1.6 kcal/mol lower; the concerted barrier is lower by 8 kcal/mol and is predicted to be the only strongly operable pathway. The closed shell pathway leading to the [6+4] endo adduct through **2X** and subsequent sigmatropic shift is calculated to be preferred over the diradical pathway by

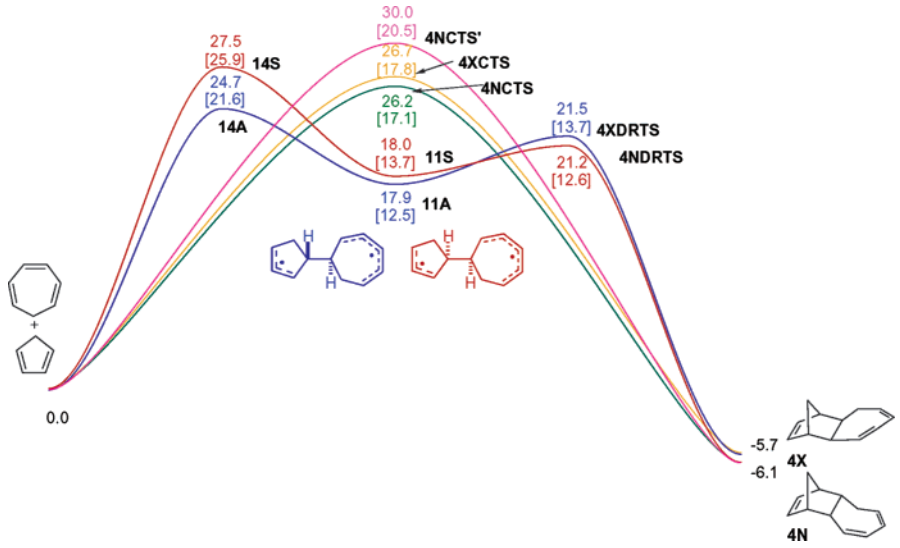

Figure 11. B3LYP/6-31G* [CASPT2/6-31G*] energetics for the cycloadditions leading to **4N** and **4X**.

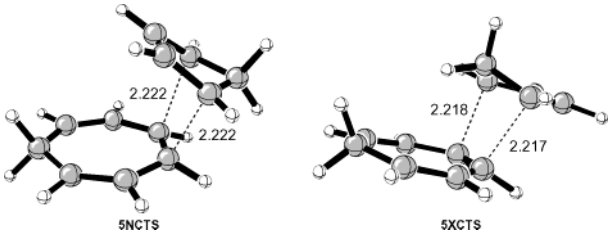

Figure 12. Concerted transition states for formation of **5N** and **5X**.

CASPT2, despite being considerably higher according to B3LYP. Both B3LYP and CASPT2 concur that the lowest [6+4] cycloaddition pathway is the concerted exo one.

2: [4+2] Cycloaddition with Cycloheptatriene as 4π Component; Two CH_2 Groups syn. RB3LYP calculations located one concerted, but extremely asynchronous transition state for this reaction: the exo transition state **2XCTS** (Figure 6). As mentioned in the previous section, the exo adduct **2X** also functions as the access route to **1N**. **2XCTS** is at 34.0 kcal/mol and has forming bond lengths of 1.993 and 3.059 Å, essentially stepwise bond formation, although it leads directly to product.

A series of constrained optimizations in which the C2−C11 and C4−C9 distances were scanned revealed that the lowest energy path between reactants and **2N** passes through alternative cycloadduct **4N** (see Supporting Information). This cycloadduct may subsequently rearrange through the [3,3] sigmatropic shift transition state **2N4NSSTS** at 28.2 kcal/mol relative to reactants. A second conformation **4NCTS′** of the transition state **4NCTS** for the concerted cycloaddition leading to **4N** was found (Figure 6). **4NCTS′** is at 30.0 kcal/mol and is intimately linked to **2N4NSSTS**. The surface permits direct passage through **4NCTS′** and **2N4NSSTS** to **2N**. Nummela and Carpenter have recently shown that even intermediates in deep wells can be bypassed by some trajectories over a surface in gas-phase dynamics calculations,[25] and this may occur in this case. This may be described as a desymmetrized bispericyclic surface, where **4NCTS′** may lead to both **2N** and **4N** without formation of an intermediate.

Unrestricted calculations on the possible stepwise pathways show that **2N** can be accessed through the syn diradical, **11S**, while the exo adduct forms via anti diradical **11A**. Thus, the stepwise endo pathway, which has its highest point at the diradical forming transition state, **14S**, is lower in energy than the concerted pathway by 2.5 kcal/mol (see Figure 7). The diradical energy is 18.0 kcal/mol, and the subsequent cyclization has a barrier of only 1.5 kcal/mol and a forming bond length of 3.04 Å in the transition state, **2NDRTS**. The stepwise exo pathway is similar and 9.3 kcal/mol lower than the concerted transition state.

The energetics for formation of **2X** and **2N** are summarized in Figure 7. The exo product **2X** is favored by B3LYP and is formed by a stepwise mechanism passing through the anti diradical, **11A**. The concerted pathways are better by CASPT2.

Significantly different outcomes are now predicted by the B3LYP and CASPT2 methods. With CASPT2, the lowest energy path is the endo cycloaddition to form **4N**, with a subsequent sigmatropic shift to give **2N**. This process involves barriers of 17.1 and 19.8 kcal/mol for the initial cycloaddition and sigmatropic shift, respectively. **4NCTS′** may also function as an access point and is close in energy, at 20.5 kcal/mol. The stepwise path through the anti diradical **11A** is calculated to have a highest point at 21.6 kcal/mol, 1.1 kcal/mol higher than **4NCTS′**. Finally, the alternative stepwise (through the syn diradical **11S**) and concerted (exo) transition states are 4−5 kcal/mol higher in energy.

3: [4+2] Cycloaddition with Cycloheptatriene as 4π Component and CH_2 Groups anti. Formation of **3** would proceed through the high energy diradicals **12S** and **12A** if the reaction were stepwise. Therefore, only concerted transition states were considered. The energies are summarized in Figure 9. The exo transition state **3XCTS** to form **3X** is quite high in energy. Adduct **3N** could only be accessed by sigmatropic shifts from **5N**, discussed below. Both **3XCTS** and the sigmatropic shift transition state, **3N5NSSTS**, are more nearly synchronous than transition states for most of the other reactions (Figure 8). This likely reflects diminished diradical character in this reaction manifold.

(25) (a) Nummela, J. A.; Carpenter, B. K. *J. Am. Chem. Soc.* **2002**, *124*, 8512−8513. (b) Nummela, J. A.; Carpenter, B. K. *J. Am. Chem. Soc.* **2002**, *124*, 14810.

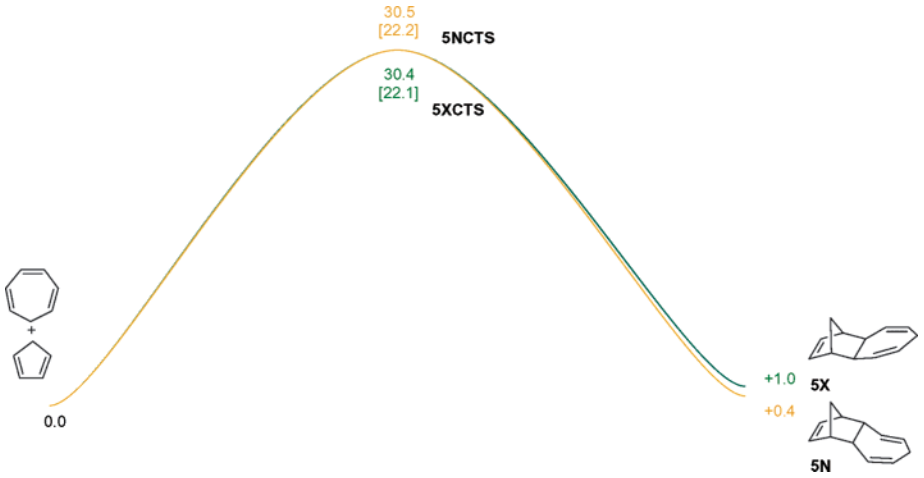

Figure 13. B3LYP/6-31G* [CASPT2/6-31G*] energetics for the cycloadditions leading to **5N** and **5X**.

4: [4+2] Cycloaddition with Cyclopentadiene as 4π Component Reacting at the External Double Bond of Cycloheptatriene. Three concerted transition states for this reaction were located: one exo and two endo. These are shown in Figure 10. The two endo transition states differ by having different conformations of the cycloheptatriene ring: one, **4NCTS**, has the ring folded away from the cyclopentadiene ring. The other, **4NCTS′**, has the two rings pushed toward one another, and this allows this transition state to be partially bispericyclic—it may lead to both **4N** and **2N** with the exact product distribution depending on the dynamic behavior of the system. This transition state was discussed in the section concerning **2N**. Like the bispericyclic transition state for the dimerization of cyclopentadiene,[9] these transition states are exceedingly asynchronous.

Two transition states for cyclization of diradicals **11A** and **11S** leading to **4X** and **4N** were located: **4XDRTS** and **4NDRTS**. These are shown in Figure 10. The five reaction paths are summarized in Figure 11. According to B3LYP the lowest energy paths are stepwise, while CASPT2 predicts that all of the concerted cycloaddition transition states are lower in energy than the transition states leading to diradical formation.

5: [4+2] Cycloaddition with Cyclopentadiene as 4π Component Reacting at the Internal Double Bond of Cycloheptatriene. Stepwise formation of **5** can only proceed through high energy diradicals, such as **12A** and **12S**. Thus the diradical paths were not considered. Two concerted transition states were obtained, both relatively synchronous (Figure 12). **5N** also serves as an intermediate en route to **3N**. B3LYP predicts this reaction to have a high barrier, related to the loss of conjugation over the course of the reaction, reflected in the endothermicity of the reaction (Figure 13).

6: [2+2] Cycloaddition (Reaction at Terminal Double Bond of Cycloheptatriene, CH_2 Groups syn). Formation of **6** is thermally forbidden and therefore must be stepwise through diradicals **11S** and **11A**. Transition states were located for the cyclization of the syn and anti diradicals (Figure 14). Both involve barriers of about 2 kcal/mol, and the anti path, leading to **6N**, is expected to be preferred. With CASPT2 single point energies this preference remains; the barriers to cyclization are low, but remain higher than for the cyclizations of diradicals which yield products of allowed reactions. There may remain some vestige of antiaromaticity in the four-membered cyclization transition state.[13] The transition state for the related cyclization of tetramethylene involves a 90 °C twist of one CH_2 terminus,[26] but that is impossible for a cyclization involving two cyclic radicals.

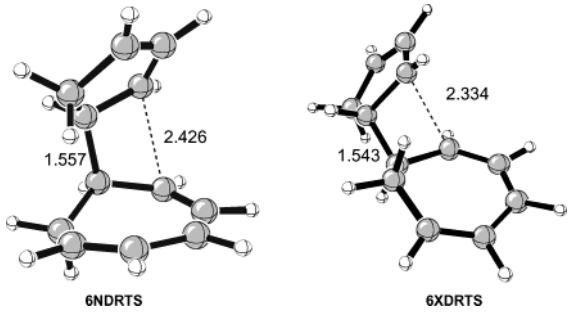

Figure 14. Transition states for cyclization of the diradicals **11A** and **11S** leading to **6N** and **6X**, respectively.

7 and 8: [2+2] Cycloadditions. Both of these reactions are forbidden and so no concerted transition states could be found. Their stepwise paths must proceed through the high energy diradicals **12S** and **12A** or **13S** and **13A**, respectively, and were not studied further.

9: [4+4] Cycloaddition. Neither endo nor exo direct cycloaddition transition states were found. These products can be formed only via [3,3] sigmatropic rearrangements from **6N** and **10N**, respectively. These two adducts themselves are formed in stepwise paths, discussed elsewhere in this paper. The sigmatropic shift transition states linking **9N** to **6N** and **9X** to **10N** were located and are shown in Figure 16. Energetics are summarized in Figure 17.

B3LYP places the second step highest, while CASPT2 predicts that the diradical formation step (**14S** or **14A**) leading to **6N** or **10N** will be the highest point on each reaction surface.

10: [6+2] Cycloaddition. This is the most exothermic reaction and consequently shows low barriers to diradical cyclization. The [6+2] adducts are formed from the diradicals with rates determined by rotation into a geometry suitable for CC bond formation: no separate barrier for diradical cyclization exists. The barriers to rotation are discussed below and described in detail in the Supporting Information. The absence of a cyclization barrier suggests the flat surface for the energetics of reaction shown in Figure 18. The thermodynamically favored

(26) Doubleday, C., Jr. *J. Am. Chem. Soc.* **1993**, *115*, 11968−11983.

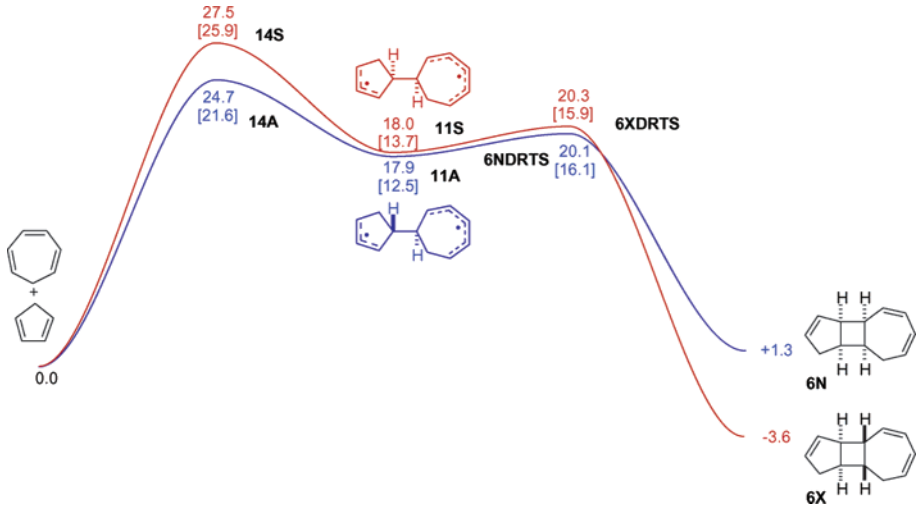

Figure 15. B3LYP/6-31G* [CASPT2/6-31G*] energetics for the cycloadditions leading to **6N** and **6X**.

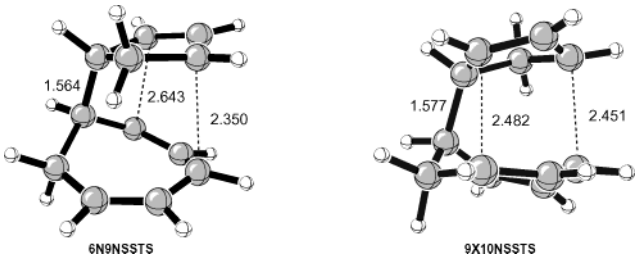

Figure 16. Sigmatropic shift transition states linking **9N** to **6N** and **9X** to **10N**.

product, **10X**, will also be the kinetically preferred product because it would arise from the cyclization of the preferred anti diradical **11A**. CASPT2 concurs with B3LYP.

Competition between Reactions Leading to Adducts 1−10. Both B3LYP and CASPT2 predict that many reactions are in competition. B3LYP predicts closely competitive diradical and concerted transition states, while CASPT2 places the concerted transition states considerably lower than stepwise reactions involving diradicals. Indeed, CASPT2 predicts that all of the allowed reaction manifolds will be dominated by closed shell concerted transition states. It is notable that all of the B3LYP values after spin projection are closer to the CASPT2 values, but the disagreement between the two methods is still large. Concerted transition states are 8.0−9.5 kcal/mol lower with CASPT2 than B3LYP, while diradical formation transition states are 1.6−3.1 kcal/mol lower, diradicals are 4.3−5.5 kcal/mol lower, and diradical cyclization transition states are 3.9−8.6 kcal/mol lower with CASPT2 than with B3LYP.

CASPT2 is generally accepted to provide a better description of the relative energies of closed and open shell structures; consequently, we expect the predictions made by this method about the relative barrier heights to be more reliable. The absolute barrier heights calculated by CASPT2 are lower than had been expected, and recent studies have shown that CASPT2 single point energies based on CASSCF geometries may be more reliable but are beyond the scope of this study.[19] The final test of which method is best for this problem will lie in comparison with experimental results.

The low barriers to cyclization found for the diradicals suggest that rotation in the diradical may be important in determining cyclization selectivity. Consistent with this, we have calculated with B3LYP that the barriers to rotation about the single bond joining the cyclopentadiene and cycloheptatriene moieties in each direction are 4.3 and 4.5 kcal/mol in **11A** and 3.7 and 5.3 kcal/mol in **11S**. (Details are given in Supporting Information.) These are higher than most of the cyclization barriers calculated with B3LYP, which range from −2 kcal/mol to 4 kcal/mol.

Conclusions

Several general conclusions can be made as a result of this study. First, we have found that, even in reactions lacking symmetry, bispericyclic procesess can occur; such two-step-no-intermediate mechanisms[27] ensure that dynamic effects may play an important role beyond what is predicted by relative barrier heights. Similarly, our CASPT2 calculations suggest that aromatic and antiaromatic labels may, although cautiously, be applied to transition states for the cyclization of diradicals.

Applying transition state theory, and neglecting products being formed through sigmatropic shifts, it is possible to calculate the product mixture predicted to be formed under kinetic control for each of the two computational methods. B3LYP predicts a mixture dominated by [6+2] adduct **10X**, formed through the diradical **11A**. The mixture comprises **10X**, **1X** (the [6+4] adduct), **4N**, **4X**, both Diels−Alder adducts, and [2+2] adduct **6N** in a ratio of 79:10:6:3:2. By contrast, CASPT2 predicts a mixture in which products arising through concerted cycloadditions are the only ones expected to be observed. A mixture of **4N**, **4X**, both Diels−Alder adducts, and **1X** ([6+4]) in the ratio of 66:20:14 is expected. Both methods agree that the product mixture will feature **1X**, the exo [6+4] cycloadduct predicted and sought by Woodward in the proposed research project of 1964, and the Diels−Alder adducts, **4N** and **4X**, involving the triene as a dienophile.

It is interesting that these predictions are reminiscent of several cycloaddition studies involving substituted dienes carried out by Houk in the Woodward laboratories in 1965−1968. The reaction of hexachlorocyclopentadiene and cycloheptatriene gives mainly the Diels−Alder corresponding to **4N**.[5] The cycloaddition of 2,5-dimethyl-3,4-diphenylcyclopentadienone

(27) Singleton, D. A.; Hang, C.; Szymanski, M. J.; Meyer, M. P.; Leach, A. G.; Kuwata, K. T.; Chen, J. S.; Greer, A.; Foote, C. S.; Houk, K. N. *J. Am. Chem. Soc.* **2003**, *125*, 1319−1328.

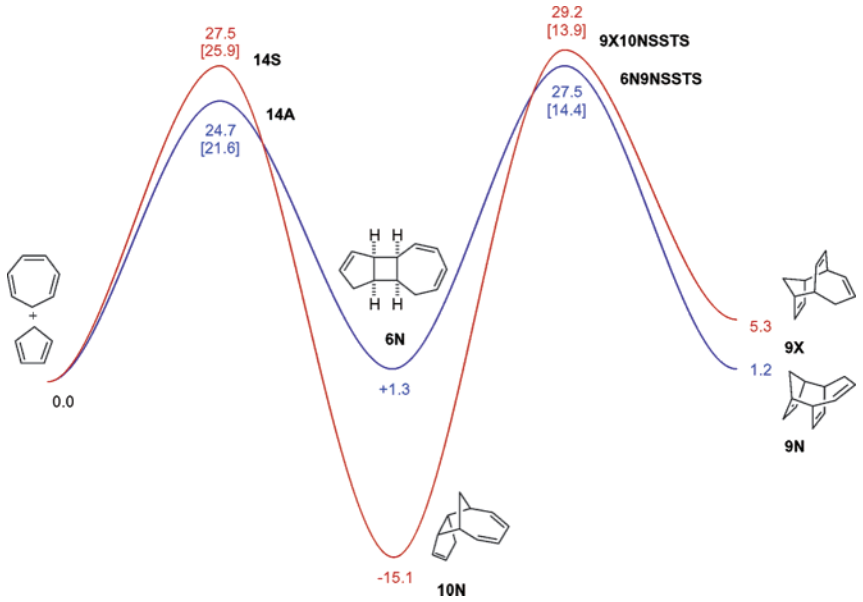

Figure 17. B3LYP/6-31G* [CASPT2/6-31G*] energetics for the cycloadditions leading to **9N** and **9X**.

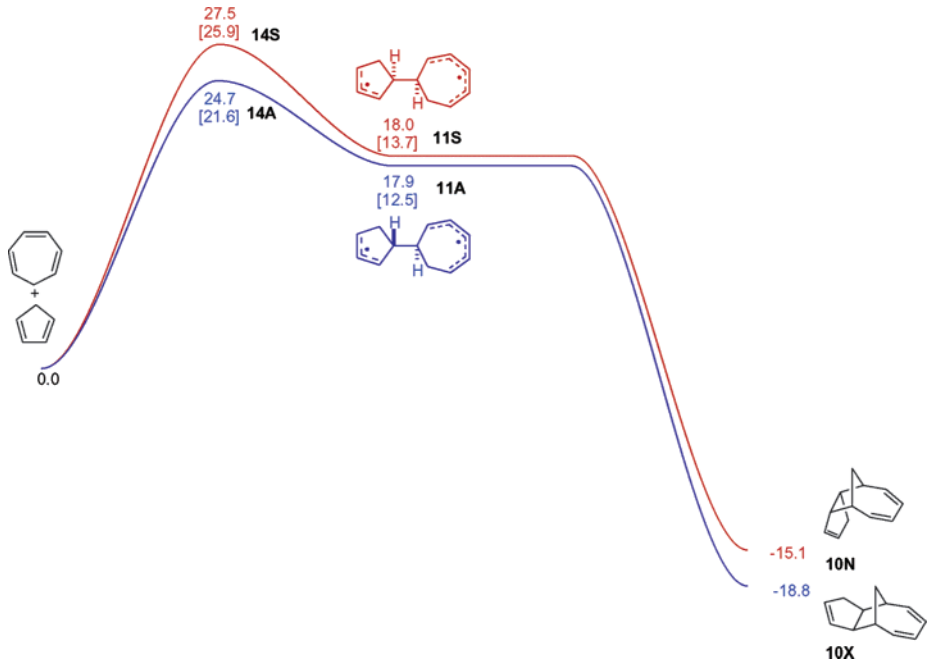

Figure 18. B3LYP/6-31G* [CASPT2/6-31G*] energetics for the cycloadditions leading to **10N** and **10X**.

yields products analogous to **1X**, **4N**, and **2N**, with the latter shown to arise from a Cope rearrangement of **4N**.[4a,5] The factors that favor **1X**, **4X**, and **4N** appear to carry over to reactions of substituted dienes with cycloheptatriene. The project proposed by R. B. Woodward has now been completed, if only theoretically. The experimental tests of these detailed predictions are still awaited.

Acknowledgment. We are grateful to the UK Fulbright Commission and AstraZeneca (for a fellowship to A.G.L.) and to the National Science Foundation and National Computational Science Alliance for financial support of this research.

Supporting Information Available: Potential energy surfaces for **1N** and **2N**. Rotational profiles, transition states, and intermediates for **11A** and **11S**. Geometries and energies for all stationary points (PDF). This material is available free of charge via the Internet at http://pubs.acs.org.

JA029694X